Supporting Information for

Synthetic Fluorescent Probes Capable of Selective Recognition of 3'-Overhanging Nucleotides for siRNA Delivery Imaging

Takaya Sato,[a] Yusuke Sato,[a*] Kenta Iwai,[b] Shusuke Kuge,[b] Seiichi Nishizawa,[a] Norio Teramae[a*]

[a]Department of Chemistry, Graduate School of Science, Tohoku University, Japan, Sendai 980-8578, Japan.
[b]Department of Microbiology, Tohoku Pharmaceutical University, Aoba-ku, Sendai 981-8558, Japan

*To whom correspondence should be addressed, E-mail: satoyuu@m.tohoku.ac.jp (YS) or teramae@m.tohoku.ac.jp (NT)

MATERIALS AND METHODS

General. RNAs were custom synthesized and PAGE purified (>97%) by Sigma-Genosys (Hokkaido, Japan). Rink Amide AM resin, Fmoc-protected amino acid derivative were purchased from Aapptec (Luisville, KY, USA). Fmoc/Bhoc protected PNA monomers were purchased from ASM Research Chemicals (Hannover, Germany). The other reagents were commercially available analytical grade and were used without further purification. The concentration of RNAs were determined from the absorbance at 260 nm measured at 85°C using the molar extinction coefficient provided by the manufacturer. Water was deionized (≥18.0 MΩ cm specific resistance) by an Elix 5 UV water purification system and a Milli-Q Synthesis A10 system (Millipore Corp., Bedford, MA, USA), followed by filtration through a BioPak filter (Millipore Corp., Bedford, MA, USA) in order to remove RNase.

Unless otherwise mentioned, all measurements were performed in 10 mM sodium phosphate buffer (pH 7.0) containing 50 mM NaCl at 20°C. Before measurements, the sample solutions containing RNAs were annealed in order to assure the formation of the siRNA duplexes as follows: heated at 75°C for 10 min, and gradually cooled to 5°C (3 °C/min), after which the solution temperature was raised again to 20°C (1°C/min).

Probe Synthesis. All probes examined in this study were synthesized on an Endeavor 90 peptide synthesizer (Aapptec, Louisville, KY, USA) based on Fmoc/Bhoc chemistry. Briefly, Fmoc-Lys(Alloc)-OH was first loaded onto Rink Amide AM resin and Fmoc/Bhoc-protected PNA monomers were then coupled. For pyrene-containing conjugates, pyrene derivative was coupled to N-terminal of the PNA-lysine assembly directly or through a glycine spacer. The assembly on the resin was performed by repetitive cycles of Fmoc deprotecting (20% piperidine in DMF), coupling with DIC/HOBt activation, and capping (acetic anhydride/pyridine). The completion of the coupling reactions was confirmed by the Kaiser test. After the selective deprotection of the Alloc group by treating with tetrakis(triphenylphosphine) palladium (0) and dimethylamine borane in dichloromethane, carboxylate-terminated butyl spacer-containing TO derivative[S1] was coupled to the ε-amino group of Lys. After the Fmoc group was deprotected, deprotection of Bhoc groups in PNA nucleotides and cleavage from the resin were carried out using a mixture of trifluoroacetic acid (TFA)/triisopropylsilane/water (95/2.5/2.5). After the resulting solution was filtered to remove the resin, the probes were then precipitated in cold diethyl ether. The crude products were purified by a reverse-phase HPLC system (pump, PU-2086 Plus x2; mixer, MX 2080-32; column oven, CO-1565 (40°C); detector, UV-2070 plus and UV-1570M (Japan Spectroscopic Co. Ltd., Tokyo, Japan)) equipped with a C18 column (Inertsil ODS3: GL Sciences Inc., Tokyo, Japan) using a gradient of water/acetonitrile containing 0.05% TFA. All probes used in this study were verified for ≥95% by MALDI-TOF-MS (4800 Plus MALDI TOF/TOF analyzer: AB Sciex, Tokyo, Japan).
AA-TO: MALDI-TOF MS for $C_{51}H_{62}N_{19}O_6S$ $[M]^+$; calcd 1068.45, found 1068.48.
Py-AA-TO: MALDI-TOF MS for $C_{70}H_{73}N_{20}O_8S$ $[M]^+$; calcd 1353.56, found 1353.93.

AA-TO and its analogues were dissolved into water to prepare the stock solutions. Stock solutions of pyrene-containing probes were prepared using water/DMSO or water/acetonitrile mixtures. These stock solutions were kept at 4°C in the dark before their use. Sample solutions of pyrene-containing probes used for the experiments contain a small amount of these organic solvents (< 0.2%).

UV-visible and fluorescence spectra measurements. Absorption and fluorescence spectra were measured using a JASCO model V-570 UV–vis spectrophotometer and FP-6500 spectrofluorophotometer (Japan Spectroscopic Co. Ltd., Tokyo, Japan), respectively. Both instruments were equipped with thermoelectrically temperature-controlled cell holders. Measurements of absorption and fluorescence spectra were done using a 2 × 10 mm quartz cell (optical path length: 10 mm) and a 3 × 3 mm quartz cell, respectively.

Conformational search of Py-AA-TO. Initially, the structure of **Py-AA-TO** was constructed in the MacroModel (ver. 9.0) software and energy-minimized using the Polak-Ribiere Conjugate Gradient (PRCG) method with Amber* force field and the GB/SA water model (convergence threshold 0.05 kJ mol^{-1} $Å^{-1}$) in order to obtain local minima. The resulting structure was subsequently subjected to 50000 steps of the Monte Carlo Multiple Minimum (MCMM) protocol in the MacroModel. The structures generated from random variation of torsion angles except amide bonds in **Py-AA-TO** were then energy-minimized with the PRCG method (Amber* force field, GB/SA water model, convergence threshold 0.05 kJ mol^{-1} $Å^{-1}$). All atoms of the pyrene and quinoline moieties in the TO unit were used for comparing a minimized structure with all previous unique minima. All structures within 10 kcal/mol of the global energy minimum were stored and analyzed by XCluster program in the MacroModel.

Fluorescence imaging of siRNA delivery in living cells. HeLa cells were grown in Dulbecco's modified Eagle medium (DMEM), 10% fetal bovine serum at 37°C in a 5% CO_2 humidified atmosphere. For the application to the analysis of siRNA delivery using polymer-based carrier (jetPRIME; Polyplus transfection, Illkirch, France), HeLa cells were seeded in a 8-chambered glass plate (Iwaki, Tokyo, Japan) at a density of 2.0×10^4 cells/well and maintained for 24 h. **Py-AA-TO** was mixed with **siGL2** in jetPRIME buffer and incubated for 20 min at room temperature in order to form the complex. For the colocalization study of **Py-AA-TO** and **siGL2**, Alexa 647-modified **siGL2** was utilized, where Alexa 647 was introduced to the middle of the **siGL2** sequences (5'-CGU ACG CGG AAU ACU UCG A dTdT-3'/3'-dTdT G CAU GCG CC (Alexa647-U) UAU GAA GCU-5') in order to assure the effective binding of **Py-AA-TO**. The aliquots of the complex (50 μL) was then mixed with jetPRIME reagent (1.75 μL), where the final concentration of **siGL2** and **Py-AA-TO** was 500 nM. Fluorescent imaging was done after addition of the resulting polyplexes onto the HeLa cells in phenol red-free medium using the DeltaVision Elite microscopy system (GE Healthcare Japan, Tokyo, Japan) consisting of an inverted microscope (Olympus IX70, Olympus, Tokyo, Japan) with a CoolSNAP HQ2 CCD camera.. All images were obtained using a 60x oil lens objective (PlanApo60, NA = 1.4, Olympus). The following filter sets were used: FITC filter set (Ex 475/28; Em 545/48) for **AA-TO**, **Py-AA-TO** and TO; TRITC filter set (Ex 545/27; Em 597/45) for ethidium bromide; and Cy5 filter set (Ex 632/22; Em 679/34) for Alexa 647. The obtained images were processed with the softWoRx software.

Examination of gene silencing activity of siRNAs. The silencing activity of siRNAs assays were evaluated using dual luciferace reporter assay system (Promega) according to the manufacturer's instructions. Briefly, the day prior to transfection, ~ 10^3 HeLa cells were plated to each well in a 96-well plate. To each well, 150 ng of pGL2 and pRuc were cotransfected with **siGL2**, **Py-AA-TO/siGL2**, and scrambled siRNA (Fasmac, 5'- AAU UCU CCG AAC GUG UCA CGU -3'/3'- UUA AGA GGC UUG CAC AGU GCA -5') using jetPRIME or Lipofectamine 2000 reagent (Invitrogen) at a final concentration of 200 nM. Luminescence intensity was recorded with SpectrtaMax M5 (Molecular Devices) after 24 h.

Statistical analysis. The measurements of siRNA silencing activity were repeated at least three times. All data were expressed as means ± SD. Statistical analysis was performed using one-way analysis of variance (ANOVA). The probability values were added within the figures. $P < 0.05$ was considered to be significant.

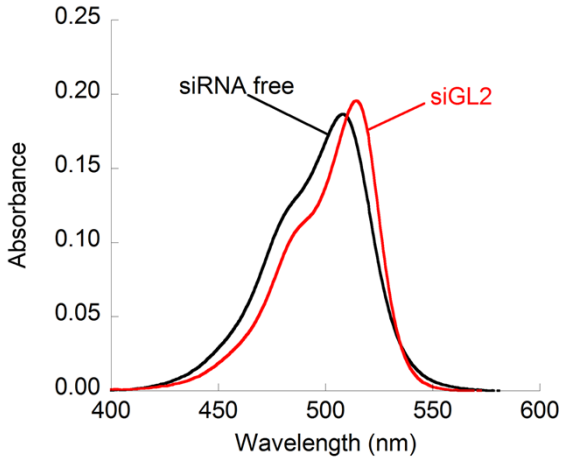

Figure S1. UV-visible spectra of **AA-TO** (2.0 μM) in the absence and presence of **siGL2** (10 μM). Other solution conditions are the same as those given in Fig. 1c in the main text. TO unit in **AA-TO** shows a slight increase in the absorbace and a redshift upon binding to **siGL2**, which indicates the intercalation of the TO unit (Ref 13a in the main text).

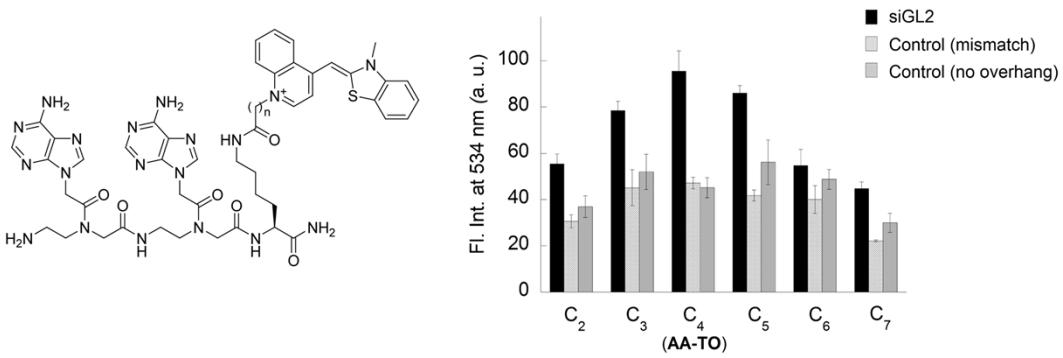

Figure S2. Effect of the spacer length in PNA-TO conjugates on the fluorescence response for the siRNAs. Conjugate analogue containing different alkyl spacers (n = 2-7) corresponds to C_n. Error bars are the standard deviations obtained from three independent experiments. Measurement conditions are the same as those given in Fig. 1c in the main text. From these results, C_4 conjugate, represented as **AA-TO**, is clarified as the best candidate due to its large and selective response for **siGL2**.

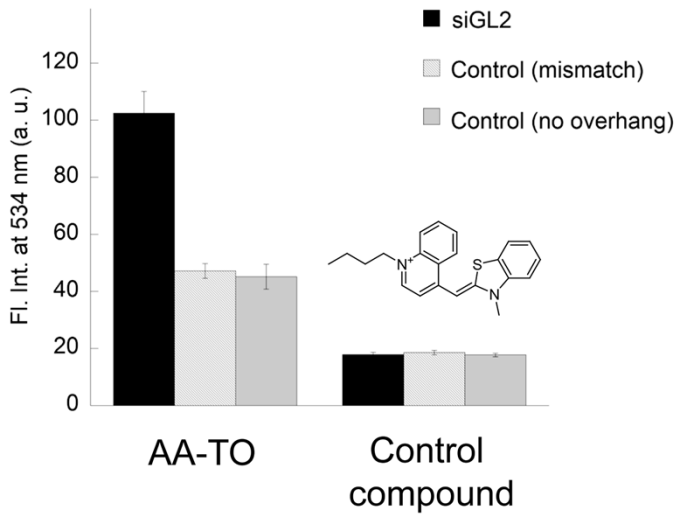

Figure S3. Fluorescence response of **AA-TO** and its control compound that lacks the PNA unit (synthesized according to Ref S1) for siRNAs. Structure of the control compound is also shown. Error bars are the standard deviations obtained from three independent experiments. Measurement conditions are the same as those given in Fig. 1c in the main text.

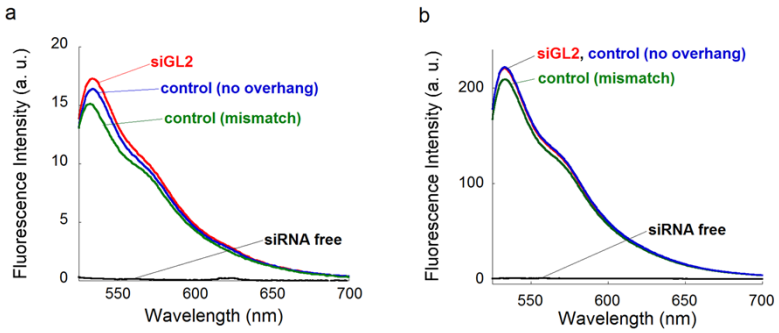

Figure S4. Fluorescence response of **AA-TO** (200 nM) for (a) equimolar (200 nM) and (b) excess amount (2.0 μM) of siRNAs. Measurement conditions are the same as those given in Fig. 1c in the main text.

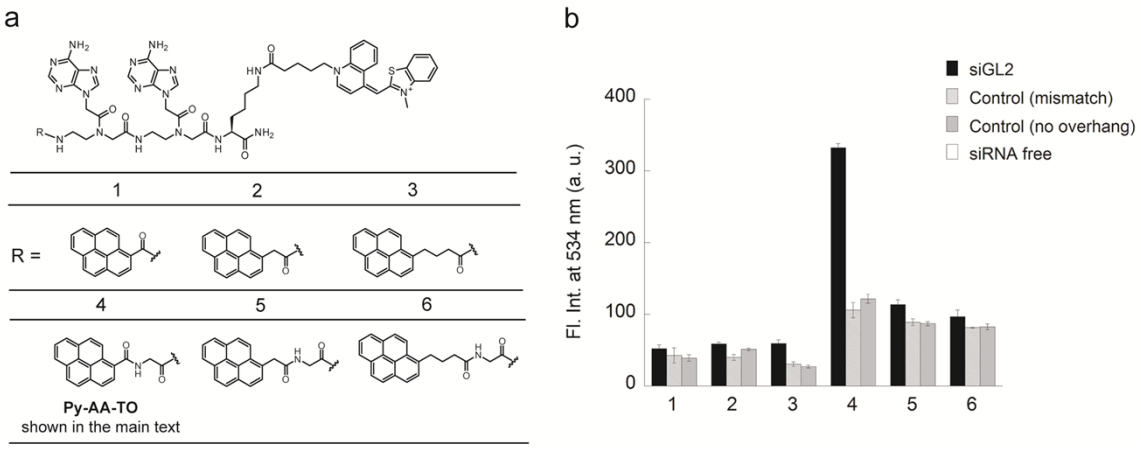

Figure S5. (a) Six kinds of pyrene derivatves examined for improved selectivity for 3'-overhanging nucleotides in siRNAs. (b) Fluorescence response of pyrene-containing **AA-TO** for the siRNAs. From the examination of six kinds of pyrene derivatives, the introduction of compound 4 into N-terminal of **AA-TO** results in highly selective response for **siGL2** over control siRNAs. The resulting probe is represented as **Py-AA-TO** in the main text. Measurement conditions are the same as those given in Fig. 2b in the main text.

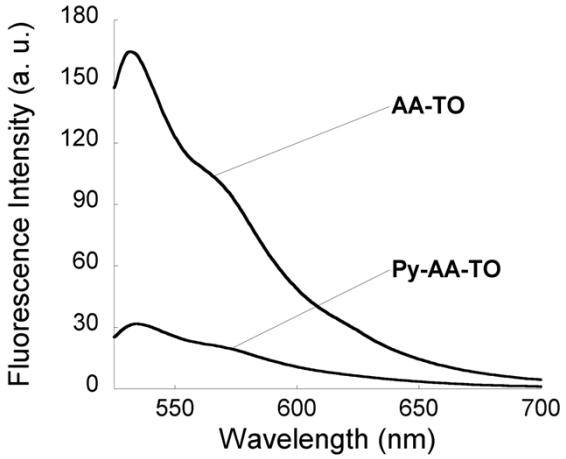

Figure S6. Comparison of fluorescence intensity of **AA-TO** and **Py-AA-TO** upon binding to **siGL2**, measured under the identical condition. Concentration conditions are the same as those given in Fig. 2b in the main text. Fluorescence intensity for **AA-TO** was larger than that for **Py-AA-TO**. This is highly likely that **AA-TO** shows non-selective binding and exhibits light-up response relative to **Py-AA-TO**.

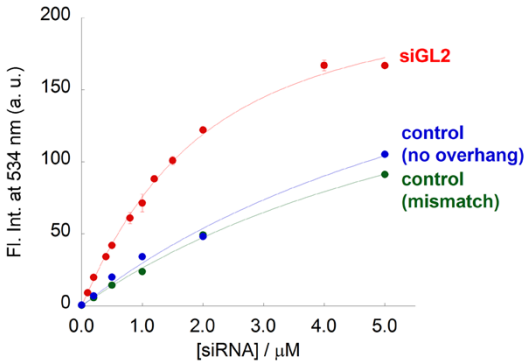

Figure S7. Fluorescence response of **Py-AA-TO** (1.0 μM) for the siRNAs (0-5.0 μM). Error bars are the standard deviations obtained from three independent experiments. Other measurement conditions are the same as those given in Fig. 2b in the main text.

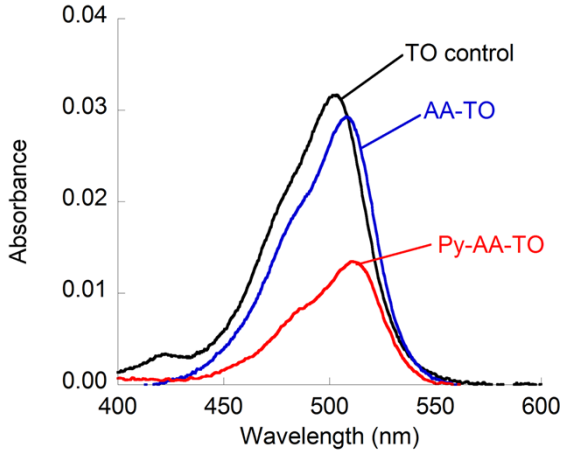

Figure S8. UV-visible spectra of **Py-AA-TO** and TO control compound (cf. Fig. S3). Absorption spectra of **AA-TO** is also shown as a comparison. The concentration of each probe is 1.0 μM. Compared to the TO control compound, absorbance of the TO unit in **Py-AA-TO** is red-shifted (10 nm) and significantly small (hypochromic effect: 58%).

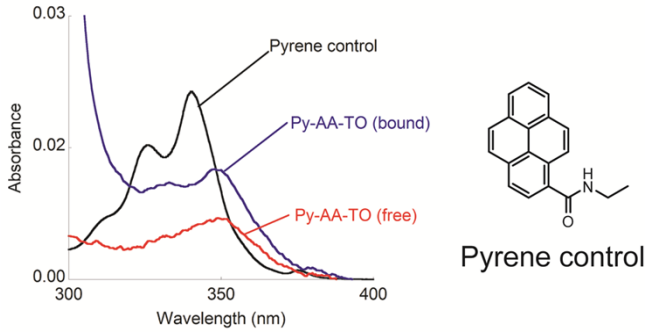

Figure S9. UV-visible spectra of pyrene unit in **Py-AA-TO** (free and bound to **siGL2**) and pyrene control compound (right: synthesized according to Ref S2). The concentration of each probe is 1.0 μM. Compared to pyrene control compound having no PNA and TO units, absorbance of pyrene unit in **Py-AA-TO** was red-shift (8 nm) and significantly small (hypochromoic effect: 70%). Vibronic structure of the pyrene unit in **Py-AA-TO** is not clearly observed due to its intramolecular stacking with the TO unit (**Figure S10**). Also, the absorbance of the pyrene unit in **Py-AA-TO** bound to **siGL2** lacks the vibronic structure, indicating the interaction between the pyrene unit and **siGL2** (Ref S3).

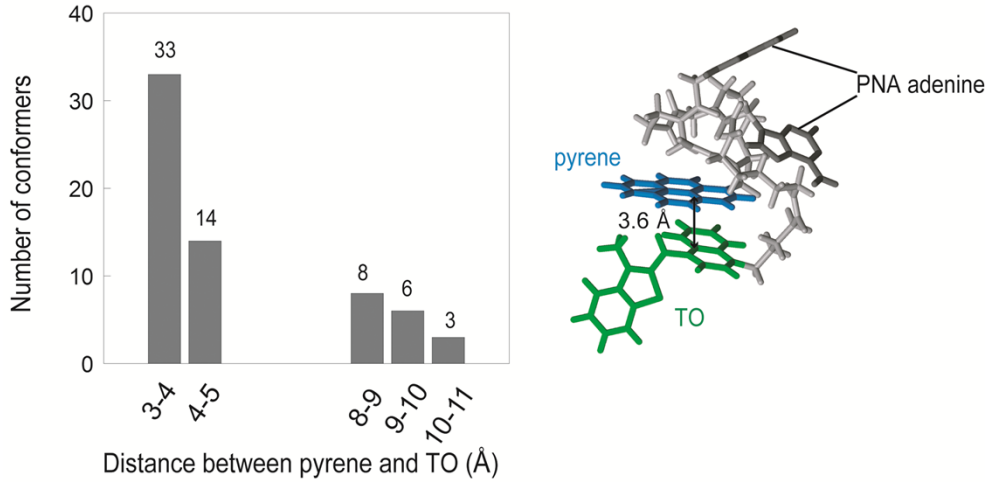

Figure S10. Conformational analysis of **Py-AA-TO** by Monte Carlo conformational search. A total of 64 conformers is identified within 10 kJ/mol of the lowest energy confomer and the distance between the quinoline ring in the TO unit and pyrene unit in the obtained conformers were then analyzed using XCluster program in the MacroModel. The largest population is clearly observed for the confomers with the distance range from 3.5 Å to 4.5 Å. The most stable confomer in this population is also shown, where the quinoline ring in the TO unit is well stacked with pyrene unit (the distance: 3.6 Å). The adaptation of such an intramolecular stacking in **Py-AA-TO** is consistent with the results in the UV-visible spectra of TO and pyrene units (cf. Figures S8 and S9).

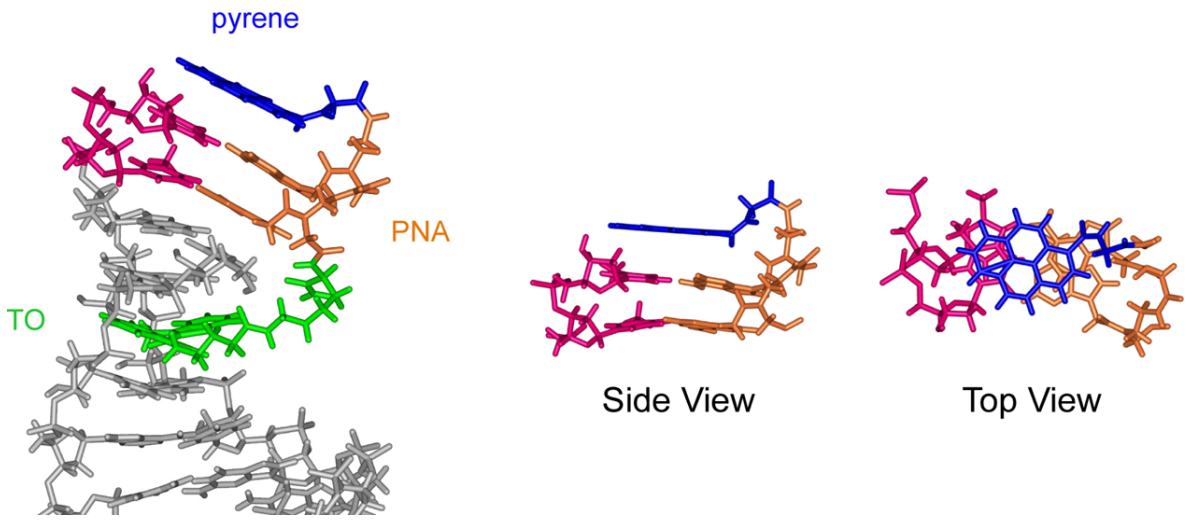

Figure S11. Molecular modeling of the binding of **Py-AA-TO** (blue, pyrene; orange, PNA adenine; green, TO) to overhanging structures of **siGL2** (pink, 2-nt overhanging nucleotides), obtained by energy minimization with MacroModel ver. 9.0 (Ref S4). To clarify the possible stacking of pyrene moiety of **Py-AA-TO** to 3'-terminal base pair, top and side views of the truncated structures are also shown.

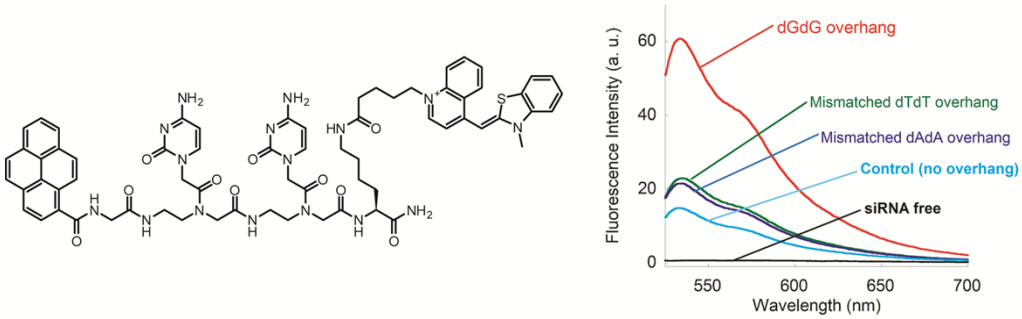

Figure S12. Structure of PNA cytosine-containing probe and its fluorescence response for 3'-overhanging nucleotides in the siRNAs (5'-CGU ACG CGG AAU ACU UCG AXX-3'/3'-XXG CAU GCG CCU UAU GAA GCU-5', X = dG, dT, dA, or none). Measurement conditions are the same as those given in Fig. 2b in the main text.

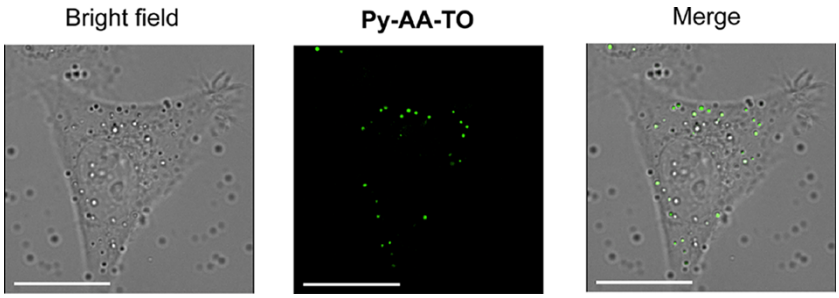

Figure S13. Analysis of siRNA (**siGL2**) delivery using **Py-AA-TO** as an affinity-labeling agent for siRNA. Images of HeLa cells were taken after being incubated with the polyplexes containing **Py-AA-TO**/**siGL2** complex (500 nM) for 3 h.

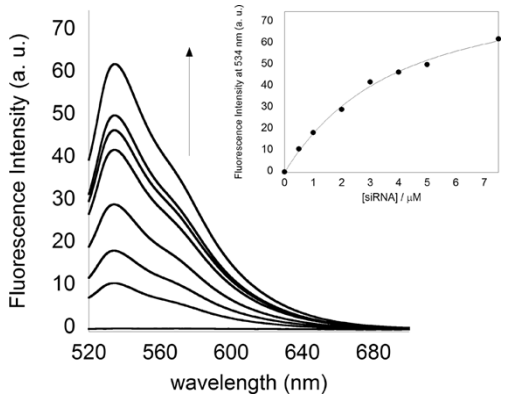

Figure S14. Fluorescence titration curve of **Py-AA-TO** for the binding to dTdT overhang in the siRNAs (5'-CGU ACG CGG A-3'/3'-dTdTG CAU GCG CCU -5'). The obtained curve was analyzed based on a 1 : 1 binding model (Ref. S5), giving the binding affinity with the dissociation constant (K_d) of 3.5 ± 0.40 μM (n = 3).

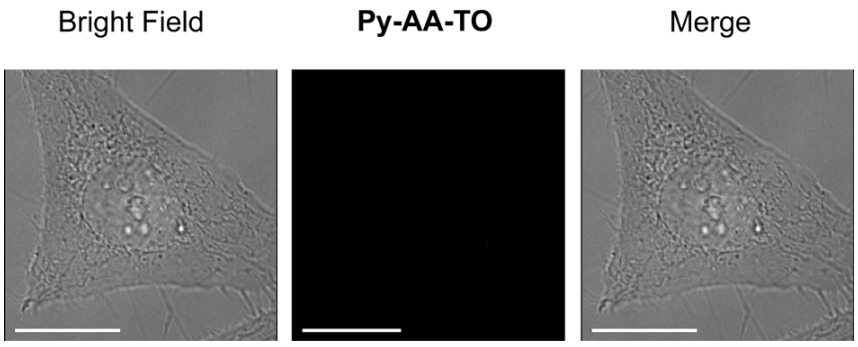

Figure S15. Images of HeLa cells treated with **Py-AA-TO** without **siGL2**. Other conditions are the same as those shown in Fig. S13.

Figure S16. Fluorescence microscope images of HeLa cells after being incubated with the polyplexes containing thiazole orange/fluorophore (Alexa 647)-modified **siGL2** complex (500 nM) for 3 h. The colocalization of two colors apprears as a yellow color. Like ethidium bromide, as shown in Fig. 3b in the main text, thiazole orange shows large fluorescence emission from non-specific binding to intracellular nucleic acids in the cytoplasm and in the nucleolus, whereas the fluorescence from thiazole orange bound to **siGL2** in the polyplexes is observed (yellow arrow). Scale bar: 20 μm.

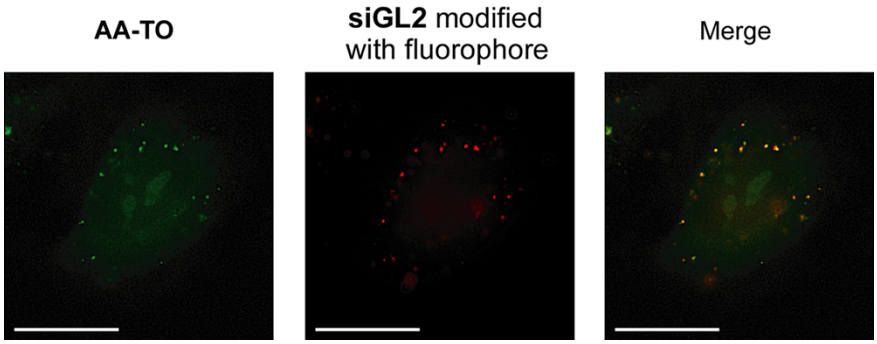

Figure S17. Fluorescence microscope images of HeLa cells after being incubated with the polyplexes containing **AA-TO** /fluorophore (Alexa 647)-modified **siGL2** complex (500 nM) for 3 h. The colocalization of two colors apprears as a yellow color. While lower than that of traditional intercalators like ethidium bromide (Fig. 3b in the main text) and thiazole orange (Fig. S16), background fluorescence of the TO unit in **AA-TO** was pronounced compared to that of **Py-AA-TO** (Fig. S13). Scale bar: 20 μm.

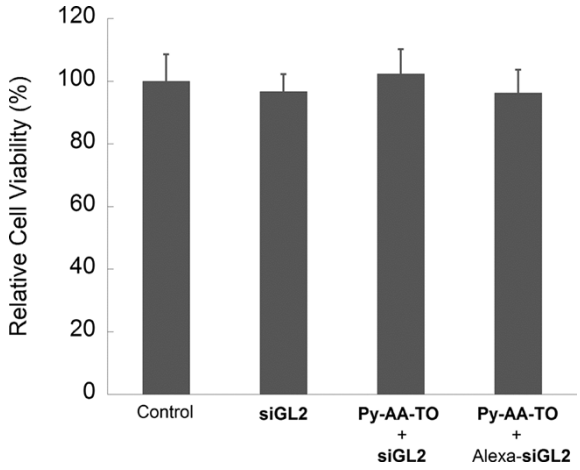

Figure S18. Cytotoxicity assessment of **Py-AA-TO**/**siGL2** and **Py-AA-TO**/ fluorophore (Alexa 647)-modified **siGL2**. HeLa cells were incubated with **PyAA-TO**/**siGL2** or Alexa 647-modified **siGL2** /jetPRIME polyplex. Also, the result using **siGL2** without **Py-AA-TO** was also shown. Buffer treatment served as a positive control. Cell viability was evaluated using alamarBlue-based assay after a 48 h incubation with **Py-AA-TO** or polyplex according to the manufacturer's instructions. Error bars represent standard deviations obtained from three independent experiments. Transfection conditions are the same as those given in Fig. 3 in the main text.

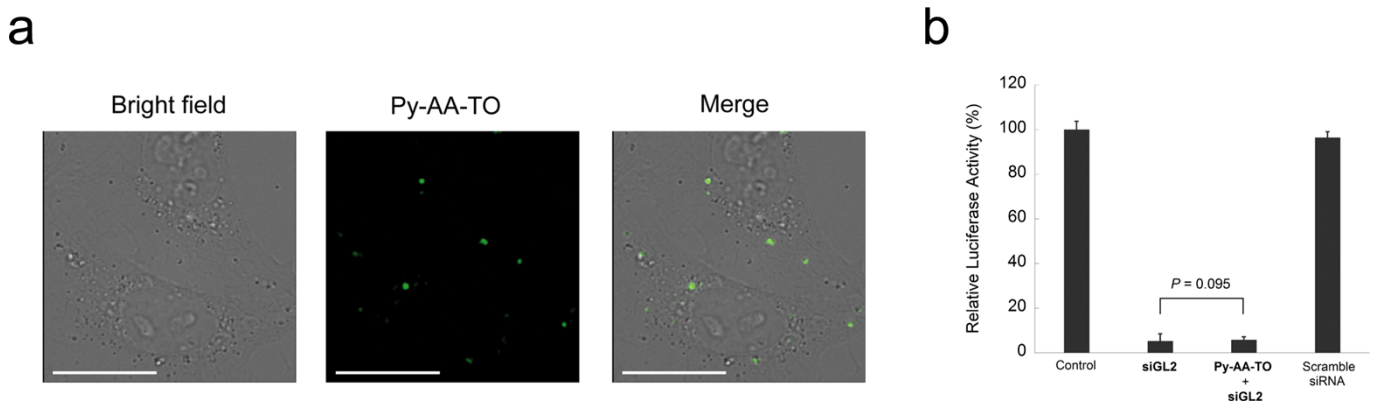

Figure S19. (a) Images of HeLa cells at 3 h after transfection of **Py-AA-TO**/**siGL2** complex (500 nM) using the lipid-based carrier (Lipofectamine 2000). Measurement conditions were the same as those given in Fig. 3a in the main text. Scale bar: 20 μm. (b) Effect of the use of **Py-AA-TO** as a siRNA affinity-labeling agent in the case of lipid-based carrier on gene silencing activity of **siGL2**. RNAi activity was evaluated using dual luciferace reporter assay system.

References

[S1] Carreon, J. R., Stewart, K. M., Mahon, Jr. K. P., Shin, S. & Kelly, S. O. *Bioorg. Med. Chem. Lett.* **17**, 5182-5185 (2007).
[S2] Hwang, J., Choi, M. G., Eor, S. & Chang S-K. *Inorg. Chem.* **51**, 1634-1639 (2012).
[S3] Siegmund, K. *et al. J. Phys. Chem. B* **113**, 16276-16284 (2009).
[S4] Sato, Y., Ichihashi, T., Nishizawa, S. & Teramae, N., *Angew. Chem. Int. Ed.* **45**, 6369-6372 (2012).
[S5] Sato, Y., Kudo, M., Toriyabe, Y., Kuchitsu, S., Wang, C-.X., Nishizawa, S. & Teramae, N., *Chem. Commun.*, **50**, 515-517 (2014).